JMEPEG (2000) 9:562-570

A Multiscale Homogenization Procedure for Analysis of Processes Involving Heat Deposition Using Constrained Parameter Optimization

S.G. Lambrakos and J.O. Milewski

(Submitted 23 January 2000; in revised form 3 May 2000)

We present aspects of a general procedure to be used in conjunction with constrained parameter optimization for the analysis of processes involving heat deposition such as welding processes and those involving rapid prototyping by means of powder deposition. Our emphasis in this report is on the construction of generating functions and subdomain elliptic solvers useful for the practical application of constrained parameter optimization for the calculation of thermal histories. The procedure for constructing generating functions and elliptic solvers is based on the concept of multiscale homogenization. We discuss those elements of the theoretical foundation of the general methodology based on constrained parameter optimization as these elements relate to the application of generating functions and subdomain solvers. In addition, we present a prototype weld analysis, which serves to demonstrate many of the details associated with the application of this methodology.

Keywords heat deposition, multiscale homogenization, parameter optimization, temperature histories, weld analysis

1. Introduction

This report is meant to provide a general description of certain aspects of a continuously evolving methodology whose purpose is the calculation of temperature histories at locations within a material during the course of a process involving heat deposition. The temperature history as a function of position within a given material is relevant in that the associated material response, in a large part, determines the structure and resultant properties of that material. This is particularly true for materials undergoing relatively rapid cooling, which is characteristic of welding or direct laser fabrication using powder where nonequilibrium solidification structures are commonly seen. The problem of calculating thermal histories, or rather, the time-dependent temperature field associated with a dynamic process involving heat deposition, is interesting in that a large fraction of the temperature field can be determined *a priori*. This can be achieved, for example, by means of distributed temperature measurements (thermocouple measurements) during the course of the process or by means of the analysis of solidification cross sections. Other types of information that could be available, *a priori*, include the volumetric shape and top surface morphology of the melt pool resulting from melting of the material. For arc welding or high energy beam welding, it is possible to estimate or measure, to some degree of accuracy, the character of the heat source depositing energy into the material. But the nature of these processes results in poor observability, making these measurements difficult and limited in accuracy. And for the case of deep penetration welding, information can be available concerning the shape and size of the vapor-liquid boundary or keyhole. The solution of the problem is therefore one where many of its aspects are readily available through common analysis. One would like to have in principle a convenient method of generating a solution that is consistent with this availability of information. It follows therefore that the idea of having a methodology where a large fraction of the solution can be embedded conveniently is well posed for this type of problem. Accordingly, we would like to adopt the basic philosophy of actually embedding most of the solution, rather than adopting procedures that generate the solution using complex mappings based on physical models that in turn could be based on relatively restrictive assumptions.

Our general methodology is based on constrained parameter optimization. We have presented over the course of different studies[1–4] various aspects of this methodology related to its mathematical framework, application to the analysis of specific types of processes, and to its continuous evolution. A significant aspect of our methodology is that model system parameters (*e.g.*, material properties), constraint conditions based on experimental information (*e.g.*, melt boundary profiles), source terms (*e.g.*, energy input, total mass melted or deposited), and boundary and bound conditions are all expressed in terms of quantities associated with system matrix elements. Within the framework of a system matrix representation, information concerning the solidification boundary and melt pool shape is of equal significance to that of information concerning the energy source and material properties. In particular, downstream information (defined relative to a moving heat source) is formally the same as upstream information. In addition, the mutual influence of any given set of matrix elements is based purely on their relative proximity within the matrix and is not biased by any model

S.G. Lambrakos, Material Science and Technology Division, Naval Research Laboratory, Washington, DC 20375-5000; and **J.O. Milewski**, Metallurgy Group, Materials Science and Technology Division, Los Alamos National Laboratory, Los Alamos, NM 87545. Contact e-mail: lambrako@anvil.nrl.navy.mil.

representation specifying their interrelationship. With respect to the system matrix, the heat conduction equation and any other of the transport equations assume the *less restrictive role of* a constraint condition on the system. The basic mathematical representation adopted in our methodology is the system matrix *itself*. Specific material properties and process parameters also assume a less restrictive role in that they are introduced in terms of adjustable parameters, which can be either adopted as fixed constraints on the system or optimized with respect to other constraints.

An interesting aspect of our methodology is that one can systematically piece together the temperature field just on the basis of bounds and consistency requirements on that field. Within the system matrix representation, one can observe the following formal equivalence. First, source term values are formally equivalent to boundary values. Second, specific physical models and boundary conditions are formally equivalent to constraint conditions. And finally, there is no formal distinction between upstream and downstream quantities relative to the dynamic weld melt pool. Typically, the mathematical properties of a given system solver (the procedure for solving the system of equations represented by the matrix) are a consequence of the manner in which the solver facilitates the transfer of information between the elements comprising the system matrix. This transfer of information is usually based on the nature of the physical process represented mathematically. The formal structure of the system matrix representation and the type of information that is typically available from weld cross section measurements provides the basis for transforming a system whose general physical character is quasi-parabolic to one which is elliptic. Further, welding processes, especially those involving deep penetration, are characterized by temperature fields having sharp transitions in scale. The elliptic formalism of our methodology provides a natural partitioning of the system, defined by a three-dimensional temperature field, into regimes that facilitate well-conditioned transitions from one characteristic length scale to another. This in turn provides for a well-conditioned optimization of the temperature field with respect to spatially distributed constraint conditions.

It is significant to note that our methodology extends the approach of constructing a solution *via* a superposition of Rosenthal-type solutions, *i.e.*, the method of distributed heat sources.[5–7] Further, our methodology does not represent an alternative to other approaches (based on specific physical models) but easily transitions to them *via* the system matrix representation. The important point, in this regard, is that one can piece together most of the solution before such a transition is effected. This can be accomplished just on the basis of bounds and consistency requirements on the solution. And finally, many of the dynamic features of a welding process are observable during the steady-state process or are actually frozen in place at the end of the weld schedule. There is a tendency to neglect the information content of these features, which can be correlated with the dynamic state of the welding process. It is this type of information that can be conveniently embedded into the system matrix and thus actually drive the solution.

Our emphasis in this report is on the construction of generating functions and subdomain elliptic solvers useful for the practical application of our methodology based on constrained parameter optimization. We present the general mathematical framework upon which our elliptic solver formalism is based. We present a discussion of aspects of the theoretical foundation of this methodology as they relate to the application of these generating functions and subdomain solvers. We extend our methodology to include a multiscale homogenization procedure for calculating temperature fields. This procedure is of particular significance for the case of welding processes, which are characterized by temperature fields having sharp transitions in scale. We present a prototype analysis of a deep penetration weld, which serves to demonstrate many of the details associated with the application of the homogenization procedure.

2. Evolution of Methodology

In this section, we discuss the evolution of our methodology. Our discussion is in terms of heuristic descriptions and schematic representations rather than a purely formal mathematical development. We present a heuristic derivation, which is motivated by the construction of a discrete system-matrix representation of the equation of heat transfer coupled to fluid convection. The model system to be specified is that of the temperature field generated by a moving heat source of a given spatial distribution either at the surface of or distributed volumetrically within a given material. The temperature field is that for energy transport in a coordinate system that is fixed in the reference frame of the moving heat source. At the initial stage of our development, the model system is defined primarily by

$$\rho(T)C_p(T)\frac{\partial T}{\partial t} + \rho(T)C_p(T)U \bullet \nabla T = \nabla \bullet [k(T)\nabla T] + \nabla \bullet q(T) + \nabla \bullet q_s(\hat{x}) \quad \text{(Eq 1)}$$

where the quantities $\rho(T)$, $C_p(T)$, and $k(T)$ are the temperature-dependent density, heat capacity, and conductivity, respectively. The quantities $\nabla \bullet q(T)$ and $\nabla \bullet q_s(\hat{x})$ are, respectively, the temperature-dependent source term and the source term associated with the input of energy into the material due to an external energy source. The quantity $\hat{x} = (x, y, z)$ is the position vector.

Referring to the grid index scheme defined by Fig. 1 and letting $T_7 = T_p$, a discrete representation of Eq 1 is given by

$$T_p = \frac{1}{w_p}\sum_{i=1}^{6} w_i T_i \quad \text{(Eq 2)}$$

where

$$w_p = \sum_{i=1}^{6} w_i \quad \text{(Eq 3)}$$

and

$$w_i = \langle \kappa_i \rangle_U + (\Delta l)\max[U \bullet \mathbf{I}_i, 0] + \delta_{i,p+1} V_B \Delta l \quad \text{(Eq 4)}$$

for $i = 1, \ldots, 6$, and

$$\kappa_i = \frac{k_i}{\rho(T_p)C_p(T_p)} \quad \text{(Eq 5)}$$

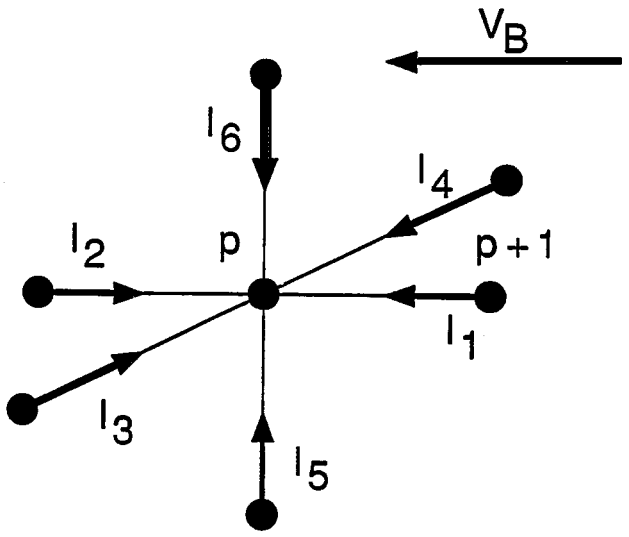

Fig. 1 Indexing scheme for unit vectors $\mathbf{I}_i$ defined by Eq 4

The quantities V_B, U, and Δl are the welding speed, fluid velocity within the melt pool, and grid resolution, respectively. The index $p = 1, \ldots, N$, where N is the total number of grid points making up the system. The unit vectors $\mathbf{I}_i$ are defined in accordance with Fig. 1. Equation 2 can be put in the form

$$\sum_{i=1}^{7} w_i T_i = 0 \qquad \text{(Eq 6)}$$

where $w_7 = -w_p$ and $T_7 = T_p$. The system of equations defined by Eq 6 can be represented by means of a system matrix:

$$\mathbf{WT} = 0 \qquad \text{(Eq 7)}$$

where

$$\mathbf{W} = \begin{pmatrix} \hat{\mathrm{w}}_1^{\mathrm{T}} \\ \vdots \\ \hat{\mathrm{w}}_{\mathrm{N}}^{\mathrm{T}} \end{pmatrix} \text{ and } \mathbf{T} = (\hat{T}_1 \cdots \hat{T}_N) \qquad \text{(Eq 8)}$$

The vectors $\hat{w}_p$ and $\hat{T}_p$, $p = 1, \ldots, N$, are such that

$$\hat{w}_p^T \hat{T}_p = 0 \qquad \text{(Eq 9)}$$

where

$$\hat{w}_p = \begin{pmatrix} w_1 \\ \vdots \\ w_7 \end{pmatrix} \hat{T}_p = \begin{pmatrix} T_1 \\ \vdots \\ T_7 \end{pmatrix} \qquad \text{(Eq 10)}$$

At this stage of our development, we review various aspects of the heuristic derivation leading to Eq 7. First, it is significant to note that although the system matrix representation defined by Eq 7 is a discrete representation of Eq 1 within the context of the above derivation, we do not adopt this as the formal interpretation of Eq 7. One should note that with respect to the system matrix representation, the heat conduction equation, itself, assumes the *subordinate role* of a constraint condition on the system. Second, we have adopted within our present development a discrete representation of Eq 1, which relates a given element T_p to six of its nearest neighbor elements, *i.e.*, Eq 2. Consequently, the vectors $\hat{w}_p$ and $\hat{T}_p$ each consist of seven elements. It should be noted that the specific type of discrete representation adopted, *i.e.*, the sizes of the vectors $\hat{w}_p$ and $\hat{T}_p$, is not relevant to our general approach. One could, for example, adopt a discrete representation of Eq 1, which relates a given element T_p to a larger number of near neighbor elements than Eq 2. The outer product defined by Eq 7 exposes the duality between the quantities $\hat{w}_p$ and $\hat{T}_p$. This duality provides the basis for adopting this formalism for application to inverse problems involving the extraction of material properties or process information from a given set of welds.

Insight is gained by examining the direct approach for mathematical analysis of the weld structure as it relates to the system matrix representation defined Eq 7. Within the context of the direct approach, all elements of the matrix **W** are assumed either known or determined *a priori* with respect to solving the system of equations defined by Eq 7. Consequently, for the direct appraoch, the quantity $\langle \kappa_i \rangle_U$, which represents a convection-weighted average of the diffusivity, is assumed determinable *a priori*. The SIMPLE algorithm[8] utilizes an explicit expression for this quantity, which is given by

$$\langle \kappa_i \rangle_U = \kappa_i \max \left[\left(1 - 0.1 \left| \frac{(\Delta l)(U \bullet \mathbf{I}_i)}{\kappa_i} \right| \right)^5, 0 \right] \qquad \text{(Eq 11)}$$

The weighting factor multiplying the diffusivity κ_l in Eq 11 considers the transition from diffusive to convective heat transfer.

One major aspect of our methodology is that of extending the concept of specifying the shape of the heat source to that of constructing the entire temperature field. This concept follows from the formal structure of the system matrix representation. Proceeding, we note that the system matrix Eq 7 can be rewritten in the form

$$W_S T_S + \sum_{I=1}^{N} W_I T_I = 0 \qquad \text{(Eq 12)}$$

where elements of the matrix $W_S T_S$ are associated with nodes that are volumetrically distributed according to the spatial profile of degree of coupling to the energy source. The sum of matrices in Eq 12 represents any general partitioning of the system matrix according to different possible physical characteristics of the elements of each matrix term. The general partitioning represented by Eq 12 exposes an important property, which contributes to the basis of our methodology. This property, stated simply, is that the set of matrix elements associated with the input of energy into the system is not formally different from any other set of elements making up the system matrix.

Another major aspect of our methodology is the concept of transforming a system whose general physical character is parabolic to one that is elliptic based on the formal structure of the matrix system representation and the type of information

that is typically available *a priori* for the process involving heat deposition. Typically, the properties of a given system solver are a consequence of the manner in which the solver facilitates the transfer of information between the elements comprising the system matrix. The type of solver selected is usually based on the nature of the physical process represented mathematically by the system matrix. The methodology considered here adopts an elliptic formalism as the basis of the "system solver," *i.e.*, the procedure for solving the system of equations represented by the system matrix. This type of formalism provides a natural partitioning into regimes, which facilitates the transition from one characteristic length scale to another. With respect to the mathematical representiion of a process involving heat deposition *via* a moving source of energy, the adaptation of an elliptic formalism is subtle in that it is counterintuitive. This is because the physical system is actually driven from upstream to downstream. That is to say, it has a parabolic character physically and as a result a parabolic solver might tend to be more intuitively satisfying. A parabolic solver, however, is not structured to facilitate the inclusion of downstream information during the process of solution generation. A system matrix representation of the discrete convective heat transfer model does not contain formal knowledge, or bias, of the parabolic character of the physical process. Solution of the system matrix can be cast in terms of an elliptic problem by simply noting that the system matrix Eq 7 can be rewritten in the form

$$W_U T_U + W_D T_D = 0 \qquad \text{(Eq 13)}$$

where elements of the matrices $W_U T_U$ and $W_D T_D$ are associated with nodes that are located upstream and downstream, respectively, relative to the heat source and that formally downstream information assumes an equivalent role to that of upstream information. This recasting of the problem is well posed for modeling heat deposition processes. This follows from the potential availability of information, *a priori*, associated with downstream regions of the temperature field for such problems and the adaptation of a methodology, which entails a construction of the entire temperature field rather than its generation by means of an upstream specification of the temperature field. It follows then that the discrete temperature field can be characterized by a global volumetric constraint of the form

$$\frac{(\Delta l)^3}{L_S} \sum_{p=1}^{N_s} \int_{T_A}^{T_p} \rho(T) C_P(T) dT = \frac{q_0}{V_B} \qquad \text{(Eq 14)}$$

rather than a relatively local constraint on the energy source defined by the energy input q_0.

There are significant advantages to applying multiscale homogenization to a system matrix representation of any physical process involving heat deposition. The method of multiscale homogenization has been the development for problems that model locally strong varying phenomena on a microscale level and that require that multiple length scales be resolved within the same solution. These problems are such that without the application of multiscale homogenization, computer storage requirements would be prohibitive relative to the appropriate grid resolution. The essence of multiscale homogenization is the determination of an approximate mathematical model that incorporates information concerning the unresolved fine-scale structure (*e.g.*, large temperature gradients in regions close to and including the heat source) of the field quantity to be determined without a strong dependence on the level of grid resolution. It follows then that a well-posed multiscale homogenization procedure requires some method of incorporating or mapping fine-scale information into a coarse scale representation. Relative to this point, it is significant to note that multiscale homogenization is conveniently adaptable to the general formalism of elliptic solvers. This follows intuitively from the nature of the type of boundary information associated with these types of solvers, which assumes more of an "interpolation" rather than "extrapolation" character. Similarly, the adaptability of multiscale homogenization with respect to our overall methodology follows from the combined use of both upstream and downstream boundary information, which assumes a interpolation character, for generation of the temperature field.

3. Generating Funtions and Subdomain Solvers

In this section, we discuss techniques for assigning values to elements of the system matrix, which is based on the construction of generating functions. Our development continues to be in terms of heuristic descriptions and schematic representations rather than a purely formal mathematical development. Our goal is to emphasize the physical basis of the various aspects of our development. The purpose of the generating function is to provide a convenient methodology for (1) assigning constraint and boundary values, (2) assigning initial estimates of values of the matrix elements, and (3) partitioning of the matrix elements into individual sets where each set of matrix elements represents a closed and bounded subdomain of the temperature field. Having constructed the system matrix by means of a generating function, the temperature field is then solved by application of an elliptic solver over those subdomains requiring local optimization of the temperature field. A generating function is defined by

$$T_G(\hat{x}) = T_A + \sum_{k=1}^{N} w_k T_k(\hat{x} - \hat{x}_k, V_B) \qquad \text{(Eq 15)}$$

$$T(\hat{x} - \hat{x}_k) = \frac{q_0}{4\pi k} \exp\left(-\frac{V_B(x - x_k)}{2\kappa}\right)$$

$$\left[\sum_{i=-\infty}^{\infty}\left(\frac{1}{R_i}\right)\exp\left(-\frac{V_B R_i}{2\kappa}\right) + \sum_{j=-\infty}^{\infty}\left(\frac{1}{R_j}\right)\exp\left(-\frac{V_B R_j}{2\kappa}\right)\right] \qquad \text{(Eq 16)}$$

$$R_i = [(x - x_k)^2 + (y - y_k)^2 + (z - 2iD - z_k)^2]^{1/2} \qquad \text{(Eq 17)}$$

$$R_j = [(x - x_k)^2 + (y - y_k)^2 + (z - 2jD + z_k)^2]^{1/2} \qquad \text{(Eq 18)}$$

where D is the thickness of the region.

The procedure of calculating the temperature field by means of Eq 15 through 18 defines the method of distributed heat sources.[9] Generating functions constructed according to this method are limited in terms of their flexibility for assigning values to matrix elements because of the assumption of temperature-independent material properties and purely diffusive

energy transfer. The method of distributed heat sources can be extended, however, by means of various lumped-parameter representations for purposes of constructing more generally applicable generating functions. It is significant to note that lumped-parameter representations, such as are given by Eq 19 and 20 below, can be directly correlated with various physical aspects of convective heat transfer resulting from a moving heat source and are therefore not strictly phenomenological. The generating function defined by

$$T_G(\hat{x}) = T_A + \sum_{k=1}^{N} w_k T_k(\hat{x} - \hat{x}_k, V_k) \quad \text{(Eq 19)}$$

provides a level of flexibility with respect to the influence of convection. The generating function defined by

$$T_G(\hat{x}) = T_A + \sum_{m=1}^{M} \sum_{k=1}^{N} w_{km} T_k(\hat{x} - \hat{x}_k, V_k, k_{km}, \kappa_{km}) \quad \text{(Eq 20)}$$

provides a level of flexibility respective to the influences resulting from the temperature dependence of material properties.

At this stage, we apply subdomain solvers. First, Eq 2 can be adopted as a coarse-scale (or average) solver for calculation of the average temperature field. It is an average solver in the sense that it is sensitive to the discreteness of the temperature field elements. Another type of solver that can be adopted is termed a homogenizing solver in that it is not sensitive to the discreteness of the temperature elements.[10] This solver is structured to include information concerning the physical character of the local variation of the temperature field as a function of position without a strong dependence on grid resolution. The general form of this solver to be adopted here is given by

$$T_{G2}(\hat{x}) = F_{G2}[T_{G1}(\hat{x})]u\,[T_{G1}(\hat{x}) - T_{G1D}] + T_{G1}(\hat{x})\,\{1 - u[T_{G1}(\hat{x}) - T_{G1D}]\} \quad \text{(Eq 21)}$$

where

$$F_{G2}(T) = \frac{(T_{G2U} - T_{G2D})\,(T - T_{G1D})}{(T_{G1U} - T_{G1D})} + T_{G2D} \quad \text{(Eq 22)}$$

The quantity $u(x)$ is the unit step function where $u(x < 0) = 0$ and $u\ (x \geq 0) = 1$.

Equation 21 establishes a mapping $[T_{G1D}, T_{G1U}] \mapsto [T_{G2D}, T_{G2U}]$. It follows then that multiple local adjustments $[T_{GND}, T_{GNU}] \mapsto [T_{GN+1D}, T_{GN+1U}]$ of the temperature field can be effected using Eq 21.

Next, we derive a solver that is adapted for the inclusion of surface tension information. It follows from the duality property given by Eq 2 that

$$w_p = \frac{1}{T_p} \sum_{i=1}^{6} T_i w_i \quad \text{(Eq 23)}$$

where T_p and T_i $(i = 1, \ldots, 6)$ assume the role of weighting coefficients. Next, it follows that if L is a linear operator, then

$$L\{w_p\} = \frac{1}{T_p} \sum_{i=1}^{6} T_i L\{w_i\} \quad \text{(Eq 24)}$$

Similarly, if Δ is a finite difference operator for application to a discrete variable defined with respect to a grid spacing Δl, then

$$\Delta w_p T_p = \sum_{i=1}^{6} \Delta w_i T_i \quad \text{(Eq 25)}$$

Referring to Fig. 1, where $U_i = \max\,[U \bullet \mathbf{I}_i, 0]$, it follows that at the top surface along the longitudinal midplane

$$\begin{aligned} &\max\,[U \bullet \mathbf{I}_1, 0] = \max\,[-u_1, 0] = 0, \\ &\max\,[U \bullet \mathbf{I}_2, 0] = \max\,[u_2, 0] = u_2 \\ &\max\,[U \bullet \mathbf{I}_3, 0] = \max\,[v_3, 0] = 0, \\ &\max\,[U \bullet \mathbf{I}_4, 0] = \max\,[v_4, 0] = v_4 \\ &\max\,[U \bullet \mathbf{I}_5, 0] = \max\,[w_5, 0] = w_5 \approx 0 \qquad \text{and} \\ &\max\,[U \bullet \mathbf{I}_6, 0] = \max\,[w_6, 0] = 0 \end{aligned} \quad \text{(Eq 26)}$$

Substituting Eq 4 into Eq 25, letting T_a, T_b, ΔU_a, and ΔU_b represent the quantities T_2, T_4, Δu_2, Δv_4, respectively, and adopting the conditions defined by Eq 26, it follows that

$$[6\Delta\kappa_p + \Delta l(\Delta U_a + \Delta U_b)]\,T_p = \sum_{i=1}^{6} \Delta\kappa_i T_i + \Delta l(\Delta U_a T_a + \Delta U_b T_b) \quad \text{(Eq 27)}$$

We note next that at the top surface, for a difference operation along the z-axis,

$$\Delta U_a = -\frac{1}{\mu}\frac{\partial\gamma}{\partial T}(T_a - T_p) \text{ and } \Delta U_b = -\frac{1}{\mu}\frac{\partial\gamma}{\partial T}(T_b - T_p) \quad \text{(Eq 28)}$$

and $\Delta\kappa_p$, $\Delta\kappa_i = 0$. Rearranging Eq 28, we obtain a discrete solver for top surface values of the temperature field given by

$$T_p = \frac{\alpha_a T_a^2 + \alpha_b T_b^2 + (\alpha_a + \alpha_b)T_p^2}{2(\alpha_a T_a + \alpha_b T_b)} \quad \text{(Eq 29)}$$

where

$$\alpha_q = -\frac{\Delta l}{\mu}\left(\frac{\partial\gamma}{\partial T}\right)_{qp} \quad \text{(Eq 30)}$$

Proceeding, we derive a solver that is adapted for inclusion of boundary-value information, which is distributed over a closed subdomain within the temperature field. For this type of domain, the level of influence due to convection is taken into account by means of the distribution of closed-surface boundary values, and as a result, Eq 2 can be replaced by

$$T_p = \frac{\sum_{i=1}^{6} \kappa_i T_i + \Delta l V_B T_{p+1}}{\sum_{i=1}^{6} \kappa_i + \Delta l V_B} \quad \text{(Eq 31)}$$

It follows then that a temperature field can be constructed that is consistent with a given set of constraints, a specified value of the objective function

$$Z_l = \left| \frac{q_0}{V_B} - \frac{(\Delta l)^3}{L_S} \sum_{p=1}^{N_S} \int_{T_A}^{T_p} \rho(T) C_p(T) dT \right| \quad \text{(Eq 32)}$$

and by adopting Eq 29 and 31 as discrete elliptic solvers. This procedure is well posed and should provide a sufficiently optimal temperature field for a range of welding processes. It is limited, however, by resolution of the grid. For a relatively coarse grid with respect to the magnitude of the temperature gradient, one can obtain a noisy temperature history at regions close to a specified closed boundary whose surface has relatively strong curvature. It is important to note that the elliptic character of the solver provides for a certain level of homogenization that is on average in that it incorporates information from both upstream and downstream fixed boundaries. This will certainly be the case at upstream regions near or at the energy source where temperature gradients are usually large and fine grid resolution is required for the generation of smooth temperature histories. One approach to this problem is the inclusion of adaptive grid procedures that adjust the resolution of the grid according to the characteristic temperature gradient within a given subdomain of the temperature field.

An alternative approach to constructing a temperature field that is consistent with a given set of constraints follows by adopting the homogenizing solver defined by Eq 21 and 22 and specified values of the objective function defined by Eq 32 and of the objective functions

$$Z_p = \left| T_p - \frac{\alpha_a T_a^2 + \alpha_b T_b^2 + (\alpha_a + \alpha_b) T_p^2}{2(\alpha_a T_a + \alpha_b T_b)} \right| \quad \text{(Eq 34)}$$

and

$$Z_p = \left| T_p - \frac{\sum_{i=1}^{6} \kappa_i T_i + \Delta l V_B T_{p+1}}{\sum_{i=1}^{6} \kappa_i + \Delta l V_B} \right| \quad \text{(Eq 35)}$$

Various features of this alternative approach are as follows. First, the homogenizing solver defined by Eq 21 and 22 generates smooth temperature histories from upstream to downstream boundary values, which are not sensitive to grid resolution. Second, information concerning material properties, *e.g.*, diffusivity and liquid metal properties, is not incorporated into the solver but rather into the associated set of objective functions. And third, this approach can be used in combination with the above approach for cases where only average trends for temperature histories are necessary within certain regions (or subdomains) while relatively exact temperature histories are required within others.

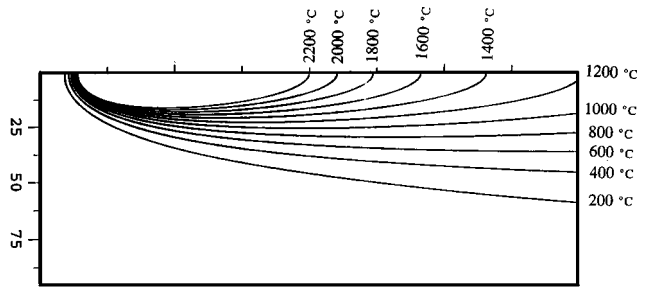

Fig. 2 Top surface plane at $z = 0$; two-dimensional slice at top surface of workpiece of three-dimensional temperature field obtained using generating function

Table 1 Welding parameters and cross-sectional information

Laser power: 9000 W	
Beam radius: 0.0006 m	
Welding speed: 0.02 m/s	
Solid/liquid boundary: Depth	Width
0 mm	1.945 mm
1 mm	1.465 mm
2 mm	0.97 mm
3 mm	0.885 mm
4 mm	0.735 mm
5 mm	0.63 mm
6 mm	0.86 mm
7 mm	1.1 mm
8 mm	1.135 mm
9 mm	1.115 mm
10 mm	1.04 mm
Melting temperature T_M: 1530 °C	
Vaporization temperature T_G: 2740 °C	

4. Prototype Analysis Using Multiscale Homogenization

In this section, we present a case study that serves to demonstrate many features of the homogenization procedure for generating a temperature field consistent with a specified number of constraints. For the present case study, we consider a prototype analysis of the deep penetration weld whose cross-sectional information and process parameters are given in Table 1. This information was taken from Reference 11. Referring to this table, three different types of information can be adopted for specifying constraints on the system. These are the transverse cross section of the solidification boundary, the rate of energy input to the workpiece, and an estimate of the shape of the keyhole vapor-liquid interface.

The first stage of the analysis entails generation of the downstream temperature field whose values are consistent with the

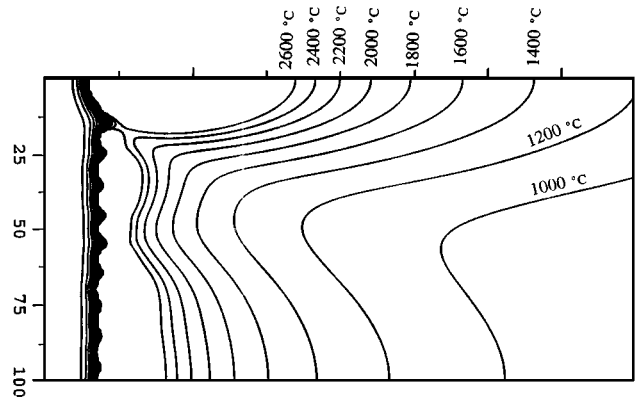

Fig. 3 Midplane at $y = 0$; two-dimensional slice at symmetry plane, parallel to direction of beam travel, of three-dimensional temperature field obtained using generating function

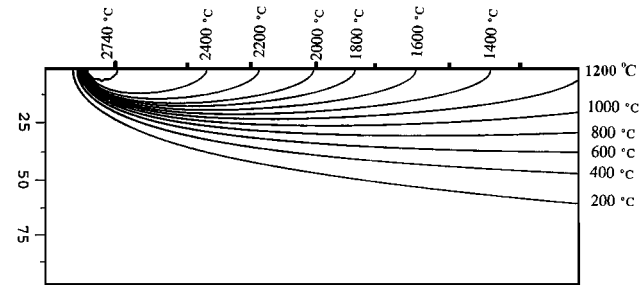

Fig. 4 Top surface plane at $z = 0$; two-dimensional slice at top surface of workpiece of three-dimensional temperature field obtained by applying homogenizing elliptic solver

solidification boundary information. This is accomplished using the generating function Eq 15 and average temperature-independent materials properties of steel. Shown in Fig. 2 and 3 are two-dimensional slices of a three-dimensional temperature field that has been constructed *via* Eq 15 such that it is consistent with the cross-sectional values given in Table 1.

The second stage of the analysis entails application of the homogenizing solver defined by Eq 21 and 22 over the closed subdomain containing all temperature values greater than T_M. Shown in Fig. 4 and 5 are two-dimensional slices of a three-dimensional temperature field that has been constructed by applying a homogenizing solver to the subdomain defined by $T > T_M$ for the temperature field shown in Fig. 2 and 3. Also shown in this figure is an isothermal surface at the vaporization temperature T_G, which has been embedded into the temperature field. This surface provides a means of embedding upstream boundary value information concerning the shape and location of the keyhole. The homogenization procedure involved local adjustments of the temperature field *via* the mappings $[T_M, 2400] \mapsto [T_M,2130]$, $[2130,3600] \mapsto [2130,2500]$ and $[2500,T_{\max}] \mapsto [2500,T_G]$, where the quantities T_M and T_G are the temperatures of melting and vaporization, respectively. The quantity $T_{\max}$ is the maximum temperature value of the temperature field obtained by the generation function.

The third stage of our analysis entails the construction of a

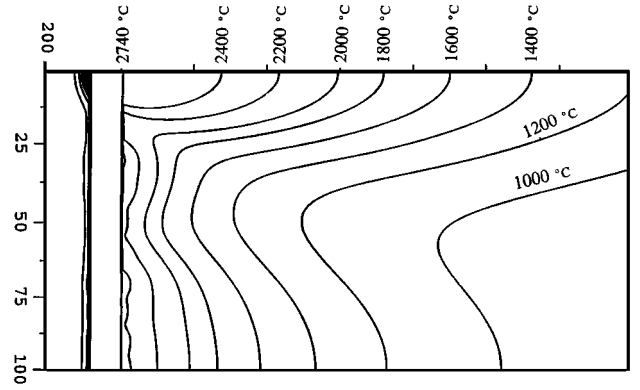

Fig. 5 Midplane at $y = 0$; two-dimensional slice at symmetry plane, parallel to direction of beam travel, of three-dimensional temperature field obtained by applying homogenizing elliptic solver

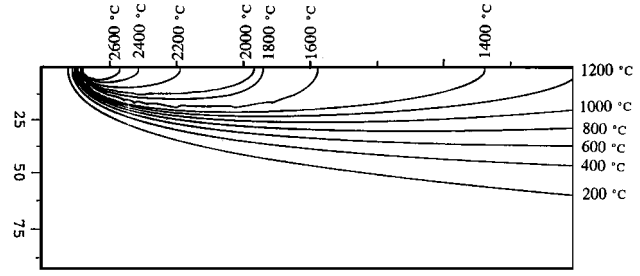

Fig. 6 Top surface plane at $z = 0$; two-dimensional slice at top surface of workpiece of three-dimensional temperature field obtained by applying discrete elliptic solver

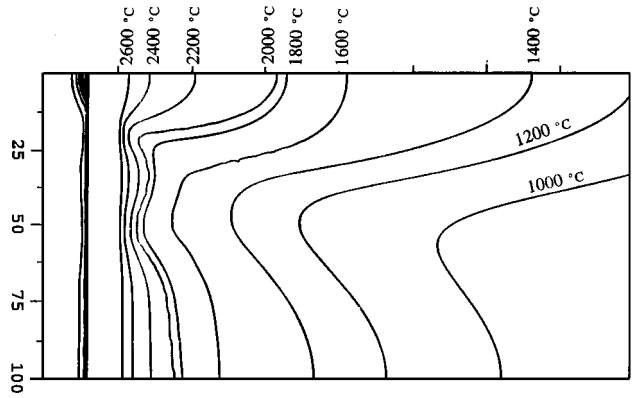

Fig. 7 Midplane at $y = 0$; two-dimensional slice at symmetry plane, parallel to direction of beam travel, of three-dimensional temperature field obtained by applying discrete elliptic solver

consistent temperature field within the upstream region of the temperature field. This is accomplished by applying the discrete solver defined by Eq 31 to the closed subdomain defined by $T < T_G$ and $T > 2100$ °C for the temperature field shown in Fig. 4 and 5. Two-dimensional slices of the resulting three-dimensional temperature field are shown in Fig. 6 and 7. Results

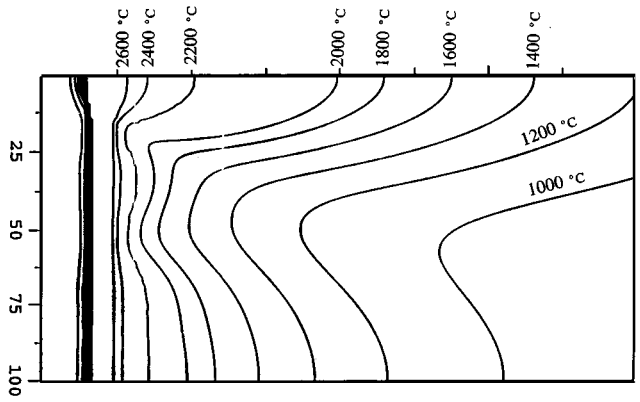

Fig. 8 Midplane at $y = 0$; two-dimensional slice at symmetry plane, parallel to direction of beam travel, of three-dimensional temperature field obtained by applying discrete elliptic solver. Shape of keyhole boundary modified to correlate with solidification boundary

of a fourth stage of the analysis are shown in Fig. 8 where the shape of the temperature-of-vaporization isotherm, along the depth of penetration, has to be changed in order to show some correlation with the observed shape of the solidification boundary. For this temperature field, the calculated value of q_0/V_B defined by Eq 14 is 3.39×10^5 J/m and the values of Z_p/T_p defined by Eq 33 and 34 are of order 10^{-6}.

The temperature field whose longitudinal slice is shown in Fig. 8 follows from the piecewise generation of a three-dimensional temperature field progressing from regions characterized by small temperature gradients to those characterized by large gradients. This piecewise construction is based on partitioning of the temperature field into closed subregions within which elliptic solvers can be adopted. With respect to this piecewise generation, generating functions serve several purposes. First, they are conveniently adaptable for calculating the temperature field at regions relatively far downstream from the energy source. Second, although they are inconvenient for calculating field values at regions relatively close to the energy source, they are conveniently adaptable to assigning values on surfaces of the specified closed subregions. And third, these provide a means of calculating "arbitrarily scaled" initial estimates of the temperature field within specified subregions for subsequent optimization *via* a homogenization solver.

For the present calculation, we have applied a discrete solver at the upstream-most regions of the temperature field. The resulting values in this region are on average homogenized due to the interpolation character of the weighting due to the closed boundary. There is, however, some noise structure superimposed on the temperature field due to the fact that the discrete solver is sensitive to the essential graininess of the boundary for a relatively coarse grid resolution. One is unable to apply a homogenization solver within this subdomain due to the essentially discontinuous distribution of sources associated with the generating function (Fig. 3). The resulting unphysical character of the temperature field is not suitable as an initial estimate for subsequent optimization *via* a homogenization solver. The homogenization procedure defined by Eq 21 and 22 is such that the initial estimate of the temperature field may be within an arbitrary scale factor of both temperature values and gradients. The initial estimate, however, must be physically consistent in that it is monotonically decreasing with distance from the region of the temperature field associated with either the surface distribution or volumetric distribution of energy sources on or within the workpiece, respectively.

The procedure for overcoming the noise structure within sudomains, which are progressively upstream relative to the energy source, is to increase local grid resolution and then apply homogenization. This approach is not to be interpreted as being equivalent to that of successive mesh embedding for the purpose of resolving highly localized structure. It is significant to note that even when used in conjunction with local grid refinement, homogenization represents the primary procedure for mapping information concerning the local variation of the temperature field as a function of position. It follows that, in general, the level of successive mesh embedding required for resolution (or smoothness) is reduced because of homogenization. In our present calculation, the application of homogenization in conjunction with increased local grid resolution could be achieved by adopting the isothermal surface defined by 2100 °C as a geometric constraint in exactly the same manner as the solidification boundary given in Table 1. For this calculation, the third stage of the analysis described above would entail generation of a discrete temperature field (*via* Eq 15) having relatively finer resolution, whose values are consistent with the boundary at 2100 °C. The homogenization solver Eq 21 could then be applied to the closed subdomain defined by all temperature values greater than 2100 °C.

5. Discussion and Conclusions

In this report, we have extended a general methodology based on constrained parameter optimization, for the analysis of processes involving heat deposition, to incorporate a multiscale homogenization procedure. In addition, we have presented a comprehensive, yet heuristic, discussion of those elements of the theoretical foundation of this methodology, as these elements relate to the application of generating functions and subdomain solvers. This is necessary in order to make clear the specific role of homogenization solvers within the overall framework of the general methodology. The specific combination of discrete elliptic solvers, *e.g.*, Eq 29 and 32, local grid refinement, and multiscale homogenization will depend on the desired level of smoothness for the temperature field with the various subdomains that make up the overall solution domain. Finally, a significant open issue for further investigation, which is motivated by the overall framework of our methodology, is the application of this methodology to inverse problems. That is the extraction of material properties or lumped process control parameters *via* the analysis of experimental data from processes involving heat deposition, *e.g.*, welding. An important aspect of our methodology, which was examined in Reference 1, is that specification of distributions of values over the boundaries of closed subdomains can be shown to be equivalent to an implicit representation of information concerning the associated heat deposition process. Significant questions related to this issue ask what are suitable explicit relationships, which could be

derived using expressions such as Eq 29 and 31, for determining material properties and process-parameter values.

Acknowledgments

The authors thank Mr. Harry N. Jones III for his discussions concerning welding processes.

References

1. S.G. Lambrakos, E.A. Metzbower, J.O. Milewski, G. Lewis, R. Dixon, and D. Korzekwa: *J. Mater. Eng. Performance*, 1994, vol. 3 (5), p. 639.
2. S.G. Lambrakos and J.O. Milewski: *J. Mater. Eng. Performance*, 1995, vol. 4 (6), p. 717.
3. S.G. Lambrakos and J.O. Milewski: *J. Mater. Eng. Performance*, 1998, vol. 7 (6), p. 1.
4. S.G. Lambrakos and D.W. Moon: *Analysis of Welds Using Geometric Constraints*, The Gordon and Breach International Series in Engineering, Technology, and Applied Science, Gordon and Breach Science Publishers, Newark, NJ.
5. H.S. Carslaw and J.C. Jaeger: *Conduction of Heat in Solids*, 2nd ed., Oxford, United Kingdom, 1959.
6. D. Rosenthal: *Weld. J. Res. Suppl.*, 1941, vol. 20, p. 220.
7. D. Rosenthal: *Trans. ASME*, 1946, vol. 68, p. 849.
8. S.V. Patankar: *Numerical Heat Transfer and Fluid Flow*, Hemisphere Publishing, New York, NY, 1980.
9. O. Grong: *Metallurgical Modeling of Welding*, Institute of Materials, London, 1994.
10. S. Knapek: *SIAM J. Sci. Comput.*, 1998, vol. 20 (2), p. 515.
11. E.A. Metzbower: *Welding Res. Suppl.*, 1990, p. 272-s.